HEATING OF SOLIDS WITH ULTRA-SHORT LASER PULSES

R. More, Z . Zinamon, K. Warren, R . Falcone, M. Murnane

JOURNAL DE PHYSIQUE
Colloque C7, supplément au n°12, Tome 49, décembre 1988

HEATING OF SOLIDS WITH ULTRA-SHORT LASER PULSES

R.M. MORE, Z. ZINAMON[1], K.H. WARREN, R. FALCONE* and M. MURNANE*

Lawrence Livermore National Laboratory, Livermore, CA 94550, U.S.A.
**University of California, Berkeley, U.S.A.*

Résumé - Cet article présente une analyse théorique du chauffage des solides par des impulsions laser ultra-courtes, de l'ordre de la femtoseconde. Les profils spatio-temporels de température sont déterminés et des techniques de diagnostic proposées. Il est possible d'obtenir des plasmas chauds avec de fortes densités, connues de manière précise. Ce qui rend possible la détermination des propriétés des matériaux dans un nouveau domaine intéressant de paramètres.

Abstract – This paper gives a theoretical analysis of the heating of solids by ultra short-pulse lasers in the femtosecond time domain. Time and space profiles of the temperature are calculated and diagnostic techniques are proposed. It is found that one can produce hot plasmas of accurately known high density, making possible the measurement of material properties in an interesting new parameter range.

1 – INTRODUCTION

The recent development of colliding-pulse mode-locked lasers opens up the possibility of performing high-power laser experiments in an ultra-fast time domain, with pulsewidths of order 10-100 fsec /1/ (1 femtosec = 10^{-15} sec). We will examine the application of such short pulse lasers to produce matter at high energy concentration combining solid state density (ρ=1 to 10 g/cm^3) with a plasma temperature (kT≈1-100 eV). The goal would be the development of experimental data that will stimulate improved fundamental understanding of hot dense matter.

For the energy densities described, theory predicts a rich assortment of phenomena including electrical conduction under conditions of short mean free paths (≃5 Å, comparable to atomic sizes), a new mechanism for electron-ion heat exchange /2/, strong changes in the range-energy relations for energetic charged particles /3/, x-ray line-shifts caused by plasma polarization /4/, and continuum shape resonances produced by pressure ionization of atomic core levels /5/. There is a great need for experiments to confirm or correct these theoretical ideas; the practical problem is the difficulty of producing well-characterized plasmas at interesting conditions.

Planar laser-interaction experiments using nsec /6/ or even psec /7/ pulses produce an expanding ablation plasma with a range of densities (.01 to 1 g/cm^3) and temperatures (1 eV to 1 keV). Theoretical calculations of the density-temperature profiles are subject to uncertainties in absorption, heat flow, radiation transfer and the nonequilibrium equation of state, all of which affect (and are affected by) the unknown density profile. Even with the most sophisticated space-time resolving diagnostics, the observed x-ray emission is a result of a range of density-temperature conditions.

Short-pulse lasers offer the possibility of a new and simpler class of experiments in which the target is heated too rapidly for hydrodynamic expansion. The plasma produced has an accurately

(1) Permanent address: Weizmann Institute of Science, Rehovot, Israel

known density, equal to its initial (solid) density, over the entire duration of the laser pulse.

The relevant characteristics of colliding-pulse mode-locked lasers with a typical pulse length $\Delta t \sim 100$ fsec$=10^{-13}$ sec are:

i) High power with a small total energy; for example, with .01 Joule focussed into a 100 micron spot one has
P=(.01 Joule)/(100 fsec) $= 10^{11}$ Watt
I=P/$(\pi(100\mu)^2) = 3 \cdot 10^{14}$ Watt/cm^2

ii) Because of the small total energy, the size and complexity of the laser remains at the modest scale typical of pure-science undertakings.

iii) The low energy lasers considered here have a high repetition rate, ca. 1 Hz, suitable for taking data in quantity with rotating disk or cylinder targets.

iv) In principle, the laser pulse itself can be used for development of equally rapid diagnostics.

Fast diagnostics are required to exploit the conditions produced by fsec lasers. In this paper we concentrate upon the measurement of reflectivity. Ng et al. /8/ used reflectivity measurements to determine the electrical resistivity of the plasma in the rarefaction wave on the back side of a laser shocked target. In this work we are dealing with reflection from the laser-target interaction region itself. Other possibilities include methods based on nonlinear mixing of copies of the main laser pulse with an output signal, gated detectors as well as the technique introduced by Mourou /9/ in which a copy of the laser pulse produces photoelectrons for electron diffraction.

For a typical sound speed $c \simeq 10^6$ cm/sec, the surface release can affect only a small depth

$$\Delta x \approx c\Delta t \approx 10^{-7} cm = 10\text{Å}$$

This is much less than the depth $\simeq$200 Å of laser heating, so most of the heated material remains at its initial solid density throughout the laser pulse.

Short-pulse lasers have been used to study melting /9/, lattice heating /10/ and phase growth /11/ in the temperature range below 0.1 eV. In this work we consider the study of electrical and thermodynamic properties in the range 1-10 eV.

In the following sections we briefly describe our understanding of the physics of laser-target interaction in the femtosecond time domain and the results of numerical calculations performed with the SPRINT code. The phenomena of interest include laser reflection and penetration into a skin depth $\simeq$200 Å, heating by inverse bremsstrahlung or Joule heating with a temperature-dependent conductivity, heat flow and ionization of the target material.

2 - OUTLINE OF A MATHEMATICAL MODEL

In this work we study the interaction with a metal of a plane-polarized laser beam at normal incidence. The interaction process considered is skin-effect absorption and Joule heating. Other laser target coupling mechanisms are less significant under conditions of interest here. Laser plasma wave instabilities coupling mechanisms require a long scale length for selection of the waves which gain from the driving field. The scale length in our case is far too short for this process to occur. Likewise, the conditions are not satisfied for resonance absorption /12/, both because of the short scale length and the assumed normal incidence of the laser beam.

The incident and reflected electronic and magnetic fields are:

$$\vec{E}_i = E_i \hat{y} e^{ikx - i\omega t}$$
$$\vec{H}_i = H_i \hat{z} e^{ikx - i\omega t}$$
$$\vec{E}_r = E_r \hat{y} e^{-ikx - i\omega t}$$
$$\vec{H}_r = H_r \hat{z} e^{-ikx - i\omega t}$$

Here the indices i and r stand for incident and reflected, respectively, and the x-axis points into the target.

From Maxwell equations the electric field of the transmitted wave E_t is described by

$$(k^2 - \frac{\partial^2}{\partial x^2})E_t = -\frac{4\pi i\omega\sigma(x)}{c^2}E_t \tag{1}$$

where σ is the ac electric conductivity of the target. At the high power levels of interest in this work Joule heating by the penetrating electric field produces a temperature profile which causes the conductivity to be dependent on x.

The boundary conditions of continuity of the (tangential) electric and magnetic fields determine the absorption and reflection processes:

$$\begin{aligned} E_t(O) &= \frac{2ik}{ik+\gamma}E_i \\ E_r(O) &= \frac{ik-\gamma}{ik+\gamma}E_i \end{aligned} \tag{2}$$

where $E_t(O)$ and $E_r(O)$ are the boundary values of the transmitted and reflected electric fields and γ is the logarithmic derivative of E_t:

$$(\frac{dE_t}{dx})_{x=0} = \gamma E_t(O)$$

We note from these expressions that the surface impedance, defined as /13/

$$Z = \frac{4\pi}{c}\frac{E_t(O)}{H_t(O)}$$

is given by

$$Z = \frac{4\pi}{c}\frac{ik}{\gamma} .$$

The reflectivity is given by

$$R = \frac{|E_r|^2}{|E_i|^2} = \left|\frac{ik-\gamma}{ik+\gamma}\right|^2$$

and the absorption coefficient is:

$$A = 1 - R$$

A qualitative picture of the field penetration and reflection is obtained by assuming x-independent conductivity, given by

$$\sigma(\omega) = \frac{n_e e^2 \tau}{m(1-i\omega\tau)}$$

Here n_e is the electron density, τ is the collision time, m is the electron mass, e the electron charge. For constant σ the field is given by

$$E(x) = E(0)e^{-x/\delta}$$

The skin depth δ is given by

$$\delta = \frac{c}{\omega_p}(1 + \frac{i}{\omega\tau})^{1/2}$$

where the plasma frequency ω_p is

$$\omega_p = (\frac{4\pi n_e e^2}{m})^{1/2}$$

The surface impedance in this case is

$$Z = -i\frac{\omega}{\omega_p}(1 + \frac{i}{\omega\tau})^{1/2}$$

In the limit $\omega\tau \gg 1$, $\omega/\omega_p \ll 1$ one obtains:

$$\delta = \frac{c}{\omega_p}$$
$$A = \frac{2}{\omega_p\tau} ,$$

independent of the laser frequency.
This limit may be a reasonable approximation in the high conductivity range of our high density targets.

The interaction process is modelled in the following way:

For a given distribution of the electrical conductivity $\sigma(x)$ the wave equation, Eq. (1), is solved subject to the boundary conditions, Eq. (2), and to the condition E→0 as X→ ∞. The numerical solution is carried out by the Numerov method /14/. The calculated electric field distribution is used to evaluate the Joule heating. The power deposition per unit volume by the beam is given by

$$P = \frac{1}{2}Re[\sigma \cdot |E|^2] = \frac{1}{2}Re[\sigma] \cdot |E|^2$$

$P \cdot \Delta t$ gives the deposited energy density in each mesh cell in a time step Δt. The equation of state is used to calculate the new distribution of temperature, and hence the new values of the electrical and thermal conductivities. The new values of the temperatures and thermal conductivities are used to calculate the heat flow during the time step. This is carried out by solving the diffusion equation, using the usual, implicit, tridiagonal scheme /15/.

3 - PHYSICAL PROCESSES AND DATA

In the model calculation described above the key material properties are the equation of state, electrical conductivity and thermal conductivity.

The equation of state used in the calculation is QEOS /16/. We mention here some relevant features. The electron contribution to the pressure and energy is calculated by the Thomas-Fermi statistical model, which is used because of its convenient scaling properties. The number of free electrons is also determined using this model. The well known problem of excessive pressure predicted by the Thomas-Fermi model at solid densities and low temperatures is handled using Barnes' empirical correction which accounts for chemical bonding at solid state /17/.

The ions contributions to pressure and energy are calculated using Cowan's /18/ analytic model which describes the ion thermal motion over the entire range of solid, liquid and gas densities and temperatures. The model uses scaling parameters which involve the Debye and melting temperatures as function of density and achieves fairly good agreement with known values of these temperatures as well as other properties such as the Gruneisen parameter. An important point is that the equation of state, being derived from a free energy formulation, is fully thermodynamically self consistent.

Treatment of non-equilibrium states with different electron and ion temperatures is possible with QEOS.

The QEOS model was extensively tested in shock wave experiments, but to date no reliable experimental data exist for the range of temperature studied here (tens of eV) at solid density.

The electrical and thermal conductivities are calculated using the conductivity model described in ref. 19. The model treats the conductivities in the solid, liquid and plasma states. The model introduces cut-off values for the electron mean free path, the screening length and

the Coulomb logarithm in the low temperature, high density region, and takes into account the known behavior of solids and liquids in that region. The results for the low temperature, high density region are very different from those of the Spitzer model /20/ which is only valid at high temperatures and low densities. The model allows for two different temperatures for the ions and the electrons in the plasma state. This conductivity model was used to obtain the dc conductivity σ_o. The frequency dependent conductivity which is required here, was obtained from the relation

$$\sigma(\omega) = \frac{\sigma_o}{1 - i\omega\tau}$$

where τ is the collision time, given by

$$\tau = \frac{4\pi\sigma_o}{\omega_p^2}$$

This approximation is strictly valid for a degenerate electron gas. It is used here, because the temperatures of interest in this work are not high compared with the Fermi temperature.

An interesting point in the calculation of the electrical conductivity is the existence of a minimum conductivity. This occurs in the model due to the assumption that the electron mean free path cannot be less than the interatomic distance. In aluminum at solid density this occurs at a temperature of about 3 eV. The possible importance of this minimum in the interaction process will be discussed later.

Radiative heat transport and radiative energy losses were not considered in this work. These are not very important at the low temperatures (10 eV) of interest here. Also, inhibition of the electron heat flow due to gradient effect was not considered at these low temperatures. The results of the calculations indicate that in this temperature range heat conduction is not a decisive factor.

In this work we assume that the electron distribution reaches equilibrium Maxwellian or Fermi-Dirac distribution. This is justified by the relatively short electron collision time (<1 fms at T=10 eV and $n_e = 10^{23}$). However, the ions remain at a much lower temperature than the electrons. In the results presented below we demonstrate and discuss the effect of the ion non-participation in the heat capacity. Equilibrium ionization is assumed in the calculations. At T=10 eV and $n_e = 10^{23}$ an ionization cross section of $\sim 10^{16}$ cm^2 is required for this assumption to be justified on a 1 fms time scale. This requirement is probably met by outer shell electrons.

4 – RESULTS AND DISCUSSION

We present results of a calculation for a particular example. The peak incident power density was 10^{14} W/cm^2. The full pulse length was 100 ps. The pulse shape was given by:

$$\mathcal{F} = F_o \; exp[-\frac{(t - 2\tau_o)^2}{\tau_o^2}]$$

and is shown in Fig. 1. The total energy in the pulse was 4.4 J/cm^2. The laser wavelength was taken to be 0.25 μm. The target was solid aluminum of thickness 600 Å. In solving for the electric field penetration into the target, the condition E=0 was prescribed at the back surface of the target (x=600 Å). The target was thick enough for this to be effectively equivalent to E$\rightarrow$ 0 at x$\rightarrow \infty$.

As mentioned above, we study the effect of ion non-equilibrium on the specific heat. We have assumed this is the main effect of the ion non-equilibrium temperature: the direct effect of the lower ion temperature on the electrical and thermal conductivities is non-significant. If the ion temperature remains $\ll T_e$, the effect on the specific heat is demonstrated in Fig. 2 which shows the temperature vs. specific energy of aluminum at solid density for ion equilibrium ($T_e = T_i$) and non-equilibrium ($T_i \ll T_e$) cases. As a result of the increased specific heat, in the non-equilibrium case the electron temperature will rise more rapidly and reach conditions of high absorption at an earlier time. This results in a higher overall absorption and larger depth of heat penetration into the target.

The time history of absorption and reflection coefficients in the cases of calculated ion equilibrium and non-equilibrium are shown in Fig. 3. It is indeed seen that in the non-equilibrium case the reflectivity drops faster from its initial high value and a state of high absorption is reached earlier.

The effect of ion non-equilibrium on the temperature profile is shown in Fig. 4. Although the peak temperatures at the target surface are not very different in the two cases, the target heats to much larger depth in the case of ion non-equilibrium.

A point of interest is the feasibility of using reflectivity measurements in order to gain information on the electrical conductivity of hot dense plasma. A possible example of a feature of the conductivity which can results in a qualitative effect is the conductivity minimum which is predicted by the model of ref. 19 to exist in the transition region between the high conductivity metallic regime and the high temperature plasma regime. It can be expected that in the beam intensity range which brings the target to conditions in which the effective temperature and density which determine the reflectivity are in the range of the conductivity minimum, a minimum in the reflectivity as a function of beam intensity will be observed.

5 - CONCLUSIONS

It has been demonstrated in the calculations of this work that ultrashort (~100 fms) laser pulses with moderate powers available with present-day technology can be used to produce hot dense plasmas at temperatures of tens of electronvolts and solid densities. These conditions are hardly obtainable by any other laboratory techniques. We have shown that a relatively simple reflectivity measurement can yield interesting information on the electrical conductivity of such plasmas. Other high speed diagnostics could be devised to study other thermodynamic and transport properties.

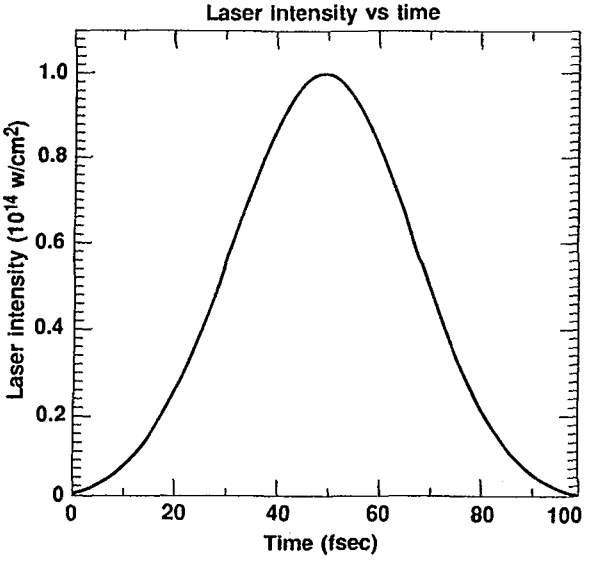

Fig. 1: Time dependence of the laser intensity used in the model calculations

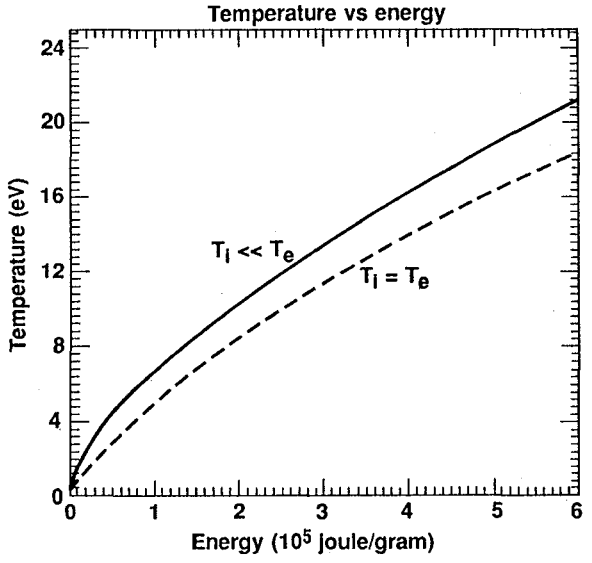

Fig. 2: Temperature of aluminum as function of specific energy in the cases of ion-electron equilibrium ($T_i = T_e$) and non-equilibrium ($T_i \ll T_e$).

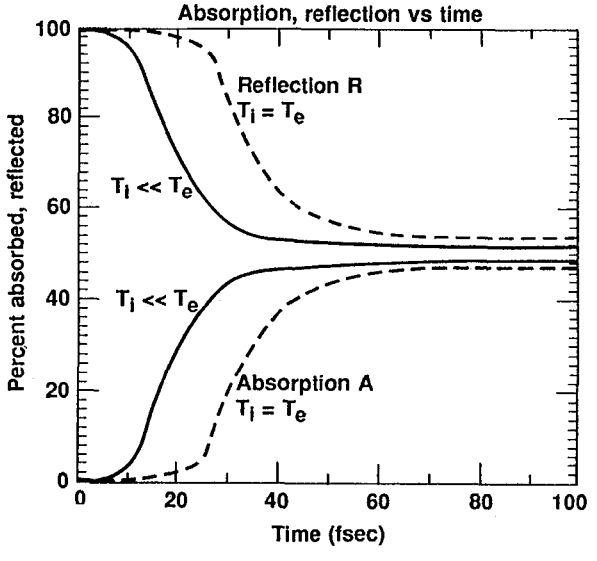

Fig. 3: Absorption and reflection coefficients of aluminum target as functions of time in the cases of ion-electron equilibrium ($T_i = T_e$) and non-equilibrium ($T_i \ll T_e$).

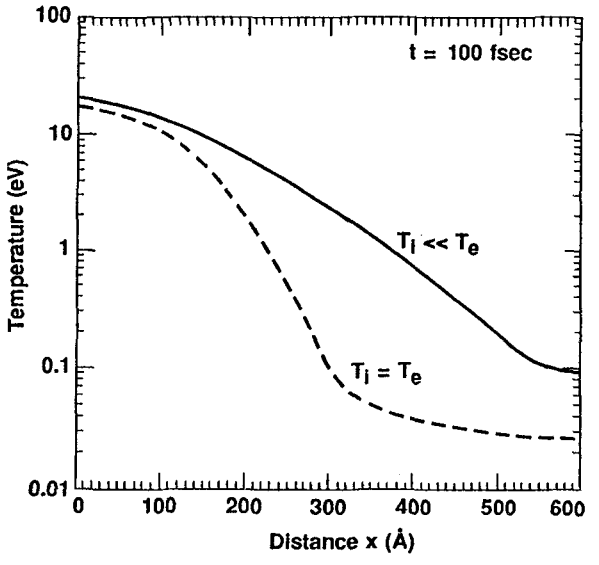

Fig. 4: Temperature profiles in the target at the end of the laser pulse in the cases of ion-electron equilibrium ($T_i = T_e$) and non-equilibrium ($T_i \ll T_e$).

REFERENCES

/1/ Fork, R.L., Greene, B.I. and Shank, C.V., Appl. Phys. Lett. 38 (1981) 671.
/2/ More, R.M., Proc. 2nd Int. Workshop on Atomic Physics for Ion Fusion, Rutherford-Appleton Lab., Chilton, Oxfordshire, UK, eds. T.D. Beynon and J.H. Aram (1984, unpublished) p. 333.
/3/ Skupsky, S., Phys. Rev. A16 727 (1977) 727; Maynard, G. and Deutsch, C.,Phys. Rev. A26 (1982) 665; Nardi, E., Peleg, E. and Zinamon, Z., Phys. Fluids 21, 578 (1978); Bailey, D.S., Lee, L.T. and More, R.M., Bull. Am. Phys. Soc.26 (1981) 900.
/4/ Griem, H.R., Spectral Line Broadening by Plasmas (Academic Press, 1974); Jaeglé, P., Jamelot, G., Carillon, A., Klisnick, A., Sureau, A. and Guennot, H., 2nd Topical Meeting on Laser Techniques in the Extreme Ultraviolet, Boulder, CO (1984).
/5/ More, R.M., Adv. At. Mol. Phys. 21 (1985) 305.
/6/ Rosen, M.D., Phillion, D.W., Rupert, V.C., Mead, W.C., Kruer, W.L., Thomson, J.J., Kornblum, H.N., Slivinsky, V.W., Caporaso, G.I., Boyle, M.J. and Tissell, K.G., Phys. Fluids 22 (1979) 2020.
/7/ Campbell, E.M., Ploeger, W.M., Lee, P.H. and Lane, S.M. Appl. Phys. Lett. 36 (1980) 12.
/8/ Ng, A., Parfeniuk, D., Celliers, P., Da Silva, L., More, R.M. and Lee, Y.T., Phys. Rev. Lett. 57 (1986) 1595.
/9/ Mourou, G., Univ. of Rochester LLE Review 24 (1985) 196.
/10/ Downer, M.C. and Shank, C.V., Phys. Rev. Lett. 56 (1986) 761.
/11/ Spaepen, F., Bull. Am. Phys. Soc. 31 (1986) 416.
/12/ Forslund, D.W., Kindel, J.M., Lee, K., Lindman, E.L. and Morse, R.L., Phys. Rev. A11 (1975) 679.
/13/ Landau, L.D. and Lifshitz, E.M., Electrodynamics of Continuous Media (Pergamon Press, 1982) p. 279.
/14/ Oset, E. and Salcedo, L.L., J. Comp. Phys. 57 (1985) 361.

/15/ Richtmyer, R.D. and Morton, K.W., Difference Methods for Initial Value Problems (Interscience, 1967).
/16/ More, R.M., Warren, K.H., Young, D.A. and Zimmerman, G.B., to be published in Phys. Fluids.
/17/ Barnes, J.F., Phys. Rev. 153 (1967) 269.
/18/ Cowan, R.D., see ref. 16.
/19/ Lee, Y.T. and More, R.M., Phys. Fluids 27 (1984) 1273.
/20/ Spitzer, L., Physics of Fully Ionized Gases (Interscience, 1962).